$$(5)\quad \mathbf{q}'\cdot\boldsymbol{\sigma}\sigma^i\otimes\sigma_i\mathbf{q}\cdot\boldsymbol{\sigma}+\sigma^i\mathbf{q}\cdot\boldsymbol{\sigma}\otimes\mathbf{q}'\cdot\boldsymbol{\sigma}\sigma_i=-2\mathbf{q}'\cdot\mathbf{q}(\delta\otimes\delta-\sigma^i\otimes\sigma_i)+\mathbf{q}\cdot\boldsymbol{\sigma}\otimes\mathbf{q}'\cdot\boldsymbol{\sigma}+\mathbf{q}'\cdot\boldsymbol{\sigma}\otimes\mathbf{q}\cdot\boldsymbol{\sigma}-2i(\delta\otimes\boldsymbol{\sigma}+\boldsymbol{\sigma}\otimes\delta)\cdot\mathbf{n},$$

$$(6)\quad \sigma^i\otimes\mathbf{q}'\cdot\boldsymbol{\sigma}\sigma_i\mathbf{q}\cdot\boldsymbol{\sigma}+\mathbf{q}'\cdot\boldsymbol{\sigma}\sigma^i\mathbf{q}\cdot\boldsymbol{\sigma}\otimes\sigma_i=-2\mathbf{q}\cdot\boldsymbol{\sigma}\otimes\mathbf{q}'\cdot\boldsymbol{\sigma}-2\mathbf{q}'\cdot\boldsymbol{\sigma}\otimes\mathbf{q}\cdot\boldsymbol{\sigma}-2\mathbf{q}'\cdot\mathbf{q}\sigma^i\otimes\sigma_i+i(\delta\otimes\boldsymbol{\sigma}+\boldsymbol{\sigma}\otimes\delta)\cdot\mathbf{n},$$

$$(7)\quad \mathbf{q}'\cdot\boldsymbol{\sigma}\sigma^i\mathbf{q}\cdot\boldsymbol{\sigma}\otimes\mathbf{q}'\cdot\boldsymbol{\sigma}\sigma_i\mathbf{q}\cdot\boldsymbol{\sigma}=-q^2(\mathbf{q}'\cdot\boldsymbol{\sigma}\otimes\mathbf{q}'\cdot\boldsymbol{\sigma}+\mathbf{q}\cdot\boldsymbol{\sigma}\otimes\mathbf{q}\cdot\boldsymbol{\sigma})+\mathbf{q}'\cdot\mathbf{q}(\mathbf{q}\cdot\boldsymbol{\sigma}\otimes\mathbf{q}'\cdot\boldsymbol{\sigma}+\mathbf{q}'\cdot\boldsymbol{\sigma}\otimes\mathbf{q}\cdot\boldsymbol{\sigma})+\delta\otimes\delta q^4+i\mathbf{q}'\cdot\mathbf{q}$$
$$\times(\boldsymbol{\sigma}\otimes\delta+\delta\otimes\boldsymbol{\sigma})\cdot n-(\mathbf{q}'\cdot\mathbf{q})^2\delta\otimes\delta+(\mathbf{q}'\cdot\mathbf{q})^2\sigma^i\otimes\sigma_i,$$

$$(8)\quad \mathbf{q}'\cdot\boldsymbol{\sigma}\otimes\mathbf{q}'\cdot\boldsymbol{\sigma}+\mathbf{q}\cdot\boldsymbol{\sigma}\otimes\mathbf{q}\cdot\boldsymbol{\sigma}=\frac{1}{2}\left[\frac{\boldsymbol{\sigma}\cdot\mathbf{P}\otimes\boldsymbol{\sigma}\cdot\mathbf{P}}{(q^2-\mathbf{q}'\cdot\mathbf{q})^2}+\boldsymbol{\sigma}\cdot\mathbf{K}\otimes\boldsymbol{\sigma}\cdot\mathbf{K}\right],$$

$$(9)\quad \mathbf{q}'\cdot\boldsymbol{\sigma}\otimes\mathbf{q}\cdot\boldsymbol{\sigma}+\mathbf{q}\cdot\boldsymbol{\sigma}\otimes\mathbf{q}'\cdot\boldsymbol{\sigma}=\frac{1}{2}\left[\frac{\boldsymbol{\sigma}\cdot\mathbf{P}\otimes\boldsymbol{\sigma}\cdot\mathbf{P}}{(q^2-\mathbf{q}'\cdot\mathbf{q})^2}-\boldsymbol{\sigma}\cdot\mathbf{K}\otimes\boldsymbol{\sigma}\cdot\mathbf{K}\right],$$

$$(10)\quad \boldsymbol{\sigma}\cdot\mathbf{n}\otimes\boldsymbol{\sigma}\cdot\mathbf{n}=-[q^4-(\mathbf{q}'\cdot\mathbf{q})^2]\sigma^i\otimes\sigma_i-\frac{1}{2}\frac{\boldsymbol{\sigma}\cdot\mathbf{P}\otimes\boldsymbol{\sigma}\cdot\mathbf{P}}{(q^2-\mathbf{q}'\cdot\mathbf{q})}-\tfrac{1}{2}(q^2+\mathbf{q}'\cdot\mathbf{q})\boldsymbol{\sigma}\cdot\mathbf{K}\otimes\boldsymbol{\sigma}\cdot\mathbf{K}.$$

PHYSICAL REVIEW VOLUME 135, NUMBER 6B 21 SEPTEMBER 1964

Breaking of SU(3) Symmetry in the $\frac{3}{2}^+$ Meson-Baryon Decuplet

K. C. WALI*
Argonne National Laboratory, Argonne, Illinois

AND

ROBERT L. WARNOCK
Illinois Institute of Technology, Chicago, Illinois

(Received 14 May 1964)

Breaking of SU(3) invariance is studied in the case of the meson-baryon decuplet with $J^P=\frac{3}{2}^+$. In a simple theory based on single-baryon exchange, the evolution of the broken decuplet from a degenerate origin is traced in detail. Symmetry breaking is introduced by allowing initially degenerate meson and baryon masses to approach continuously their physical values, while obeying at every stage the Gell-Mann–Okubo sum rules. The following conclusions are reached: (i) The Okubo equal spacing rule for the decuplet levels follows from the validity of the Gell-Mann–Okubo rules for the meson and baryon octuplets. (ii) The main effect of the symmetry breaking may be characterized as a mixing of the 10- and 27-dimensional representations. The mixing is small enough so that the resonances can be unambiguously associated with the 10 representation, but at the same time large enough to imply coupling-constant ratios differing appreciably from the values for pure symmetry. (iii) In the approach to pure symmetry through reduction of mass differences, there are no difficulties of the type pointed out by Oakes and Yang. Resonances cross thresholds smoothly, and a degenerate decuplet of bound states is obtained in the limit.

1. INTRODUCTION

MESON-BARYON resonances with $J^P=\frac{3}{2}^+$ have been assigned tentatively[1] to the (3,0) decuplet representation of the group SU(3).[2] The resonant states in question are $N_{3/2}^*$ (1238 MeV, $T=\frac{3}{2}$, $Y=1$), Y_1^* (1385 MeV, $T=1$, $Y=0$), $\Xi_{1/2}^*$ (1530 MeV, $T=\frac{1}{2}$, $Y=-1$). It now appears likely that these states all have the correct $\frac{3}{2}^+$ spin-parity values.[3] To complete the decuplet, a particle Ω_0 (sometimes called Ω_-) with $T=0$, $Y=-2$ was predicted. The recent discovery[4] of such a particle constitutes strong evidence for both the decuplet assignment and the general scheme of the "eightfold way."[2] The discovery is all the more remarkable, since the observed mass (1686 ± 12 MeV) of Ω_0 agrees very well with the prediction of the Gell-Mann–Okubo mass formula.[2,5] For the (3,0) decuplet, the

* Work performed under the auspices of the U. S. Atomic Energy Commission.

[1] R. E. Behrends, J. Dreitlein, C. Fronsdal, and B. W. Lee, Rev. Mod. Phys. **34**, 1 (1962); S. Glashow and J. J. Sakurai, Nuovo Cimento **26**, 622 (1962); M. Gell-Mann, *Proceedings of the 1962 International Conference on High Energy Physics at CERN*, edited by J. Prentki (CERN, Geneva, 1962); R. Cutkosky, J. Kalckar, and P. Tarjanne, Phys. Letters **1**, 93 (1962); R. H. Capps, Nuovo Cimento **27**, 1208 (1963).

[2] M. Gell-Mann, Phys. Rev. **125**, 1067 (1962); California Institute of Technology Report CTSL-20, 1961 (unpublished); Y. Ne'eman, Nucl. Phys. **26**, 222 (1961).

[3] A summary of the experiments and a bibliography is given by R. H. Dalitz, Ann. Rev. Nucl. Sci. **13**, 339 (1963).

[4] V. E. Barnes, P. L. Connolly, D. J. Grennell, B. B. Culwick, *et al.*, Phys. Rev. Letters **12**, 204 (1964). We prefer the notation Ω_0 to Ω_-, since the isotopic spin has been used as a subscript for the other decuplet states. The Ω_0 notation appears also in Ref. 7.

[5] S. Okubo, Progr. Theoret. Phys. (Kyoto) **27**, 949 (1962).

latter implies that the masses should be a linear function of Y; i.e., that they should be equally spaced.

The agreement of experiment with this equal spacing rule, as well as the agreement of the pseudoscalar meson and baryon masses with the analogous rule for the octuplet representation, deserves close scrutiny from the theoretical side. Gell-Mann and Okubo assume that the perturbation which upsets SU(3) symmetry has the transformation properties of the $T=0$, $Y=0$ member of an SU(3) octuplet, and that departures from symmetry can be calculated as first-order effects of this perturbation. Although this hypothesis results in a good description of mass splittings within the 0^- and $\frac{1}{2}^+$ octuplets and the $\frac{3}{2}^+$ decuplet, one should still ask whether it will be sufficient to describe *all* major departures from strict SU(3) symmetry. For example, may the perturbations of coupling constants be calculated along the same lines as mass perturbations? Putting the matter another way, the sense in which the perturbation is to be regarded as weak needs clarification.

In this paper, we study the symmetry breaking of the decuplet in several of its aspects. Our method is to regard the mass splittings within the decuplet as a direct consequence of the mass splittings within the meson and baryon octuplets. For the latter, we insert the observed masses. This procedure is carried out within a simple theory in which the meson-baryon composite states of the decuplet are produced by single-baryon exchange forces. The theory amounts to a simplification of the model used by Martin and Wali.[6] The simplification is mainly the recognition that the meson and baryon mass differences have their strongest influence in centrifugal barrier effects. With an appropriate choice of coupling parameters, the observed decuplet mass splittings can be reproduced. Thus, without using a perturbation method to calculate the splittings, we conclude that the validity of the mass formulas for the meson and baryon octuplets implies the validity of the formula for the decuplet. This confirms a result of Tarjanne and Cutkosky[7] which is based on a similar model, but on a relatively rough calculation. We also show that from an appropriate point of view the perturbation can be regarded as weak, at least in the problem of mass shifts. Specifically, the off-diagonal perturbations of the initially diagonal D matrix can almost be neglected. On the other hand, when we calculate the perturbations of the coupling constants of decuplet states to their constituents, we find that the perturbation can no longer be regarded as weak. The departures from pure symmetry are pronounced, and show very little resemblance to the formulas of Dullemond, Macfarlane, and Sudarshan.[8] The departures from symmetry are such as to improve the agreement with experiment, particularly with regard to the branching ratio of Y_1^* decays. An alternative way to judge the degree of symmetry breaking is to calculate all transition amplitudes in the basis of those states which, in their degenerate limits, transform according to pure group representations. Evaluation of such amplitudes at the resonance energies shows that group invariance arguments are quite adequate to predict which amplitudes will be large and which small. However, the relative magnitudes of small amplitudes are not well predicted. The amplitudes to which we refer are T matrix elements divided by the initial and final momenta.

In order to trace the development of the broken multiplet from its degenerate origin, we perform a gradual reduction of the meson and baryon mass differences, while maintaining the corresponding Gell-Mann–Okubo relations. As one expects, the Okubo relation for the decuplet is satisfied with more and more precision as the symmetry breaking is reduced. The degenerate level is a bound state with a binding energy of about one pion mass. The coupling constant ratios do not approach their pure symmetry values very rapidly.

We are especially concerned with some criticisms of the decuplet assignment raised by Oakes and Yang.[9] These authors have posed the following questions: (i) If one imagines that the symmetry breaking perturbation is gradually reduced, can the poles representing the decuplet states move in some reasonably simple way to arrive at a common real or complex energy in the degenerate limit? (ii) Is there any theoretical basis for applying the Okubo formula to the decuplet? (iii) Is the symmetry breaking slight enough so that group invariance arguments are meaningful? Our answer to the first two questions is yes, contrary to the contentions of Oakes and Yang. With regard to question (iii), our model shows clearly that group considerations do play a useful role. However, group arguments must be used with caution, particularly in the derivation of coupling constant ratios.

In Sec. 2 we review the structure of the Riemann surface of the many-channel scattering matrix. The ND^{-1} representation is employed.[10] An examination of the motion of poles as symmetry breaking is reduced shows that when a resonance crosses a threshold there are inevitably two poles at complex energies near that threshold. One lies on the sheet reached from the physical sheet by crossing the cut above the threshold, and the other on the sheet reached by crossing the cut below the threshold. One pole causes the resonance peak when the peak is above the threshold, and the other,

[6] A. W. Martin and K. C. Wali, Phys. Rev. **130**, 2455 (1963).
[7] P. Tarjanne and R. E. Cutkosky, Phys. Rev. **133**, B1292 (1964); see also S. Frautschi, Phys. Letters **8**, 141 (1964).
[8] C. Dullemond, A. J. Macfarlane, and E. C. G. Sudarshan, Phys. Rev. Letters **10**, 423 (1963); see also E. C. G. Sudarshan, *Proceedings of the Athens Topical Conference on Recently Discovered Resonance Particles* (Ohio University Press, Athens, Ohio, 1963). *Note added in proof*. The formulas of Dullemond *et al.*, have been criticized recently by V. Gupta and V. Singh (to be published).
[9] R. J. Oakes and C. N. Yang, Phys. Rev. Letters **11**, 174 (1963).
[10] R. L. Warnock, Nuovo Cimento **32**, 255 (1964).

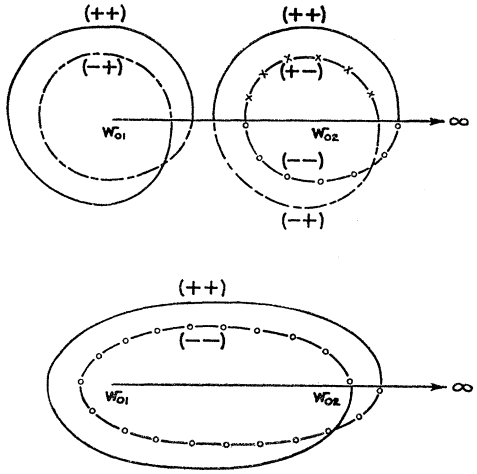

FIG. 1. Diagrams of the course of a point moving over the Riemann surface of a two-channel scattering matrix. The plus and minus signs indicate the four different sheets through which the point may move, as explained in the text.

when it is below. In this conclusion we agree with many other authors who have discussed the problem in different formalisms.[11] In Sec. 3 our model and some methods of calculation are described. Section 4 contains the main results of a numerical evaluation of the theory. We tabulate resonance energies, coupling constants, matrix elements, and so on. In the Appendix a fictitious two-channel problem is analyzed in order to illustrate more concretely the behavior of poles. The model involves a resonance which is first located between the two thresholds, and which crosses the upper threshold as the perturbation is turned off. There is a pair of complex conjugate poles on each of the three unphysical sheets. A calculation shows that the poles have nearly the same position on all three sheets, so it is indeed appropriate to refer to the poles as "shadows" of one another.[12]

2. THE RIEMANN SURFACE AND THE MOTION OF POLES

We are concerned with spin-0 particles scattered from spin-$\frac{1}{2}$ targets, so it is appropriate to work in the complex plane of w, the energy in the center-of-mass frame.[13] We neglect channels with more than two particles. In the w plane, a single partial-wave scattering matrix $T(w)=[T_{ij}{}^{\gamma}(w)]$, $\gamma=(J,T,Y)$, yields both orbital states $l=J\pm\frac{1}{2}$ corresponding to a given total angular momentum J. T has left and right "physical" branch cuts $(-\infty,-w_0)$ and (w_0,∞), where w_0 is the energy of the lowest state having quantum numbers γ. We denote these cuts collectively by the letter P. By MacDowell's relation,[13]

$$f_{l=J-1/2}(w)=T(w+i0), \quad w>w_0,$$
$$f_{l=J+1/2}(w)=-T(-w-i0), \quad w>w_0, \qquad (2.1)$$

where T has been normalized so that in the single-channel case $f_l(w)$ reduces to $f_l=\sin\delta_l\exp(i\delta_l)/q$; here q is the center-of-mass momentum. The structure of the Riemann surface is very clearly brought out by means of the matrix ND^{-1} representation.[14] Suppressing the index γ, we have $T=ND^{-1}$, where $N=[N_{ij}(w)]$ is analytic in a region including the physical cuts P, and[15]

$$D_{ij}(w)=\delta_{ij}-\frac{w-\hat{w}}{\pi}\int_P\frac{\rho_i(w')N_{ij}(w')dw'}{(w'-\hat{w})(w'-w)}=\delta_{ij}+I_{ij}. \qquad (2.2)$$

The factor ρ_i is equal to the i channel momentum for $|w|$ greater than the i-channel threshold, and is zero otherwise.

$$\rho_i(w)=q_i(|w|)\theta(|w|-w_{0i}). \qquad (2.3)$$

Because of the analyticity of $N(w)$ around P, we learn all about the sheets which are connected along P by direct inspection of Eq. (2.2). For the problem at hand we are concerned only with the $p_{3/2}$ state, which is associated with the right physical cut (w_0,∞). Each row of the D matrix has just two sheets which are connected by this right cut. We denote these two sheets by the symbols $(+)$ and $(-)$. The representations of the ith row of D on these two sheets are

$$D_{ij}{}^{(+)}(w)=\delta_{ij}+I_{ij}(w),$$
$$D_{ij}{}^{(-)}(w)=\delta_{ij}+2iq_i(w)N_{ij}(w)+I_{ij}(w), \qquad (2.4)$$

where $j=1,2,\cdots n$ and I_{ij} is given by Eq. (2.2). Taking into account $q_i(w+i0)=-q_i(w-i0)$, $w>w_{0i}$, it is easy to check that $D_{ij}{}^{(+)}(w\pm i0)=D_{ij}{}^{(-)}(w\mp i0)$. Since $D_{ij}{}^{(+)}$ and $D_{ij}{}^{(-)}$ are both analytic in the cut plane, it follows that one is the analytic continuation of the other, and that only two sheets of D_{ij} are connected through the right cut. Thus, if there are n channels, T has 2^n sheets connected through the right cut, corresponding to all possible choices for the rows of the D matrix.

In the two-channel case the situation can be visualized easily in the diagram shown in Fig. 1. The notation for sheets follows a suggestion by Yang.[16] Sheet $(+-)$

[11] M. Ross, Phys. Rev. Letters **11**, 450 (1963); R. J. Eden and J. R. Taylor, Phys. Rev. Letters **11**, 516 (1963); M. Nauenberg and J. C. Nearing, *ibid.* **12**, 63 (1964); R. H. Dalitz and G. Rajasekaran, Phys. Letters **5**, 373 (1963); G. Rajasekaran, Nuovo Cimento **31**, 697 (1964); C. R. Hagen, Phys. Rev. Letters **12**, 153 (1964); D. Amati, Phys. Letters **7**, 290 (1963).

[12] R. J. Eden and J. R. Taylor, Phys. Rev. **133**, B1575 (1964).

[13] S. W. MacDowell, Phys. Rev. **116**, 774 (1960); W. R. Frazer and J. R. Fulco, *ibid.* **119**, 1420 (1960); G. Frye and R. L. Warnock, *ibid.* **130**, 478 (1963).

[14] J. D. Bjorken, Phys. Rev. Letters **4**, 473 (1960).

[15] We neglect the possibility that "unphysical" branch points (i.e., those not associated with unitarity in the direct channel) might lie on the physical cuts P. This neglect is not really justified in all the problems treated in this paper; for example, the branch point associated with two-pion exchange in $\bar{K}$-N scattering appears above the π-Λ threshold in all $T=1$, $Y=0$ amplitudes. This problem can be overcome by deforming the paths of integrals in the D matrix so as to dodge the branch points. The model described in Sec. 3 has no such branch points.

[16] C. N. Yang, Proceedings of the Argonne User's Group (to be published).

is the sheet obtained by taking $D_{1j}^{(+)}$ for the first row of D and $D_{2j}^{(-)}$ for the second, and so on. Three other diagrams like that of Fig. 1 may be drawn, since the solid curve can correspond to any one of the four sheets. Now suppose there is a resonance above the upper threshold w_{02}. We make the usual assumption that it is represented by a pole on the sheet reached from the physical sheet by crossing the cut above w_{02}; i.e., there is a pole on sheet $(--)$, near the real axis. If the parameters of the theory are altered so that the resonance moves to a different energy, can it cross the threshold w_{02}? The Y_1^* pole must undergo such a crossing as the decuplet passes to its degenerate limit. If the resonance lies at an energy between w_{01} and w_{02}, it must correspond to a pole on sheet $(-+)$. As Oakes and Yang pointed out, a pole can move continuously from $(--)$ to $(-+)$ only by making a clockwise circuit around w_{02} through the sheet $(+-)$. Such a complicated pole motion seems unlikely, particularly if one expects that the motion of poles can be calculated as a first-order effect of a symmetry-breaking perturbation. Fortunately, the pole need not travel from $(--)$ to $(-+)$, since there is already a different pole on $(-+)$ which takes over to represent the resonance when the latter moves below w_{02}. To show that this new pole is practically inevitable, we note that all poles of T near the physical cut are given by zeros of $\det D$. Let w_R be the position of the original pole on $(--)$: $\det D^{(--)}(w_R)=0$. As $\mathrm{Re}(w_R)$ decreases through w_{02}, $\det D^{(--)}(w_R)$ and $\det D^{(-+)}(w_R)$ become nearly equal, since they differ only by terms involving $q_2(w_R)N_{2j}(w_R)$ as a factor. The explicit formulas are

$$\det D^{(-+)}=(1+2iq_1N_{11}+I_{11})(1+I_{22})-(2iq_1N_{12}+I_{12})I_{21},$$

$$\det D^{(--)}=(1+2iq_1N_{11}+I_{11})(1+2iq_2N_{22}+I_{22})-(2iq_1N_{12}+I_{12})(2iq_2N_{21}+I_{21}).$$

In the case of a narrow resonance crossing the threshold we have $\mathrm{Re}(w_R)=w_{02}$ and $q_2(w_R)\simeq q_2(w_{02})=0$. Therefore, the function $\det D^{(-+)}(w)$ must have a zero at a point very close to w_R. Note that the resultant pole of T on $(-+)$ is quite distinct from the pole on $(--)$, since these two sheets are not directly connected. The same mechanism operates if the resonance crosses a threshold moving upward. Also, the inclusion of additional two-particle channels causes no difficulty. The calculations described in the following confirm this behavior of poles. Not only do we have the poles that are necessary to allow resonances to cross thresholds; we also expect poles on *all* of the unphysical sheets, since the various determinants differ only by small terms. The pole positions on all of the sheets are calculated explicitly in the two-channel model treated in the Appendix.

3. DESCRIPTION OF THE MODEL

As remarked in the Introduction, we assume that the forces responsible for the $J^P=\frac{3}{2}^+$ decuplet are mainly due to baryon exchanges in meson-baryon scattering. For given isotopic spin and hypercharge, we retain only the coupled two-particle channels and construct the matrix ND^{-1} representation for the partial-wave scattering matrix $G(w)$. G is related to the $J=\frac{3}{2}$ partial-wave T matrix defined in the previous section by $G_{ij}=T_{ij}/q_iq_j$. For the matrix N we take the Born approximation for single baryon exchange computed with degenerate masses. Thus, N has the form

$$N(w)=h(w)N_0. \tag{3.1}$$

N_0 is an energy-independent matrix, consisting of Yukawa-type meson-baryon coupling constants given by exact SU(3) symmetry. Thus, N_0 depends on only two parameters—a parameter that determines the $D-F$ mixing ratio[2,6,17] and an over-all coupling constant $g^2/4\pi$. The elements of N_0 can be found from the SU(3) coupling constants and the isotopic spin factors given in Ref. 6 (Appendixes I and II). The energy-dependent factor $h(w)$ is a single function defined by

$$h(w)=\frac{1}{16\pi w}\left\{\frac{1}{E-M}[A_1+(w-M)B_1]+\frac{1}{E+M}[-A_2+(w+M)B_2]\right\},$$

where

$$A_l=-g^2\frac{M-M_i}{q^2}Q_l(x);\quad B_l=\frac{g^2}{q^2}Q_l(x),$$

$$x=1+[2(M^2+m^2)-M_i^2-w^2]/2q^2,$$

$$E\pm M=[(w\pm M)^2-m^2]/2w. \tag{3.2}$$

Q_l denotes the Legendre function of the second kind. The masses of the meson, the external baryon, and the exchanged baryon are m, M, and M_i, respectively. E is the baryon energy, so the squared center-of-mass momentum is $q^2=(E+M)(E-M)$. The rationalized coupling constant is denoted by g.

In computing $h(w)$ we take $m=m_\eta$, $M=M_\Lambda$, and a mass larger than that of Λ for the exchanged baryon: $M_i=10.5m_\pi c^2$. The Λ and η masses represent the Gell-Mann–Okubo degenerate limits for the baryon and meson masses in the absence of the SU(3) symmetry breaking interactions. The rather large mass for the exchanged baryon is a device to move the real axis branch points of the Born approximation to the left of the lowest threshold of the problem (viz., the π-N threshold), while keeping the η and Λ masses for the external lines. By this device we make N analytic on the right, and thereby avoid spurious difficulties which have to do only with the artificial assumption of degenerate masses in N. The N constructed this way actually has a behavior on the right cut roughly similar to that of the Born matrix evaluated with physical masses throughout.

[17] R. E. Cutkosky, Ann. Phys. (N. Y.) 23, 415 (1963).

The D matrix takes the form

$$D(w)=1-\frac{w-\hat{w}}{\pi}\int_P \frac{\rho(w')h(w')dw'}{(w'-\hat{w})(w'-w)}N_0, \quad (3.3)$$

where ρ is a diagonal matrix with elements

$$\rho_{ij}(w)=\delta_{ij}q_i^3(|w|)\theta(|w|-w_{0i}). \quad (3.4)$$

The subtraction point $\hat{w}$ lies in the interval $(-w_0,w_0)$; its value has an influence on the effective strengths of the left singularities, and thereby on the positions of resonances and bound states predicted by the theory. The "centrifugal barrier" factor $\rho(w)$ is computed from the physical masses in the case of full symmetry breaking, or from nondegenerate masses with smaller splittings as the symmetry breaking is decreased. The way in which the symmetry breaking parameter x is introduced is discussed in the next section. The symmetry violation in the present model is due only to $\rho(w)$ and the factor q_iq_j in $T_{ij}=q_iq_jG_{ij}$, which is also computed from degenerate masses. Therefore, our model attributes a higher symmetry to the N matrix than to the D matrix. This may have some general validity, but as far as numerical results are concerned it reproduces those of Ref. 6 in which N was calculated with physical masses. In this sense it is a justifiable simplification especially suited to investigate the questions mentioned earlier.

In the limit of exact SU(3) symmetry, each meson-baryon state specified by isotopic spin T and hypercharge Y can be expressed in terms of the eigenstates that correspond to the irreducible representations of $8\otimes 8$. For a set of coupled two particle channels, there exists a unitary transformation U between the definite particle states and the states that transform by SU(3) representations. The matrix N_0 is diagonalized by U, so that

$$U^\dagger N_0 U=\Lambda, \quad (3.5)$$

where $\Lambda=[\lambda_i\delta_{ij}]$. Further, from

$$G=ND^{-1}=h(w)\times\left[N_0^{-1}-\frac{w-\hat{w}}{\pi}\int_P \frac{\rho(w')h(w')}{(w'-\hat{w})(w'-w)}dw'\right]^{-1}, \quad (3.6)$$

it follows that

$$U^\dagger GU=h(w)\left[\Lambda^{-1}-\frac{w-\hat{w}}{\pi}\int_P \frac{U^\dagger\rho(w')Uh(w')}{(w'-\hat{w})(w'-w)}dw'\right]^{-1},$$
$$=h(w)[E(w)]^{-1}. \quad (3.7)$$

The requirement that the scattering matrix be symmetric is satisfied in our approximation scheme, as is evident from Eq. (3.6).

Bound states and resonances correspond to zeros of $\det E$ on the appropriate sheets of that function, as explained in Sec. 2. To investigate the zeros of $\det E$, we introduce ρ_0, which is the unit matrix times $q_0^3(|w|)\theta(|w|-w_0)$, where q_0 and w_0 are the momentum and the threshold, respectively, for the "unperturbed" meson and baryon masses m_η and M_Λ. Then

$$E(w)=\Lambda^{-1}+I_0(w)+\Delta(w), \quad (3.8)$$

where

$$I_0(w)=-\frac{w-\hat{w}}{\pi}\int_P \frac{\rho_0(w')h(w')dw'}{(w'-\hat{w})(w'-w)} \quad (3.9)$$

is the unperturbed unitarity integral and

$$\Delta(w)=-\frac{w-\hat{w}}{\pi}\int_P \frac{(U^\dagger\rho U-\rho_0)(w')h(w')dw'}{(w'-\hat{w})(w'-w)} \quad (3.10)$$

represents the symmetry-breaking perturbation. If the perturbation Δ is zero, the determinant factors:

$$\det(\Lambda^{-1}+I_0)=(\lambda_1^{-1}+I_0)\times(\lambda_2^{-1}+I_0)\cdots(\lambda_n^{-1}+I_0). \quad (3.11)$$

Each factor corresponds to one of the representations contained in the direct product $8\otimes 8$. In this case of pure symmetry, the coupling constant and the $D-F$ mixing parameter can be chosen so that the factor corresponding to the $\frac{3}{2}^+$ decuplet vanishes at some bound state or resonance energy w_0^*, and so that the other factors do not vanish at any energy that would be reasonable for a resonance or bound state. Now when Δ is included, the numerical evaluations reported in the next section show that the determinant still factors to a fairly good approximation. We have

$$\det E=\det(\Lambda^{-1}+I_0+\Delta)\simeq(\lambda_1^{-1}+I_0+\Delta_{11})\times(\lambda_2^{-1}+I_0+\Delta_{22})\cdots(\lambda_n^{-1}+I_0+\Delta_{nn}). \quad (3.12)$$

The off-diagonal elements of Δ do not contribute appreciably, and in this sense *the perturbation is weak.* The same choice of mixing parameter that was used in the degenerate case still guarantees that only the $\frac{3}{2}^+$ decuplet factor vanishes.

In calculating positions of resonances or bound states, we are concerned with $\det E(w+i0)$, w real, where the limit is taken from the physical sheet. A bound state corresponds to $\det E(w+i0)=0$, and a narrow resonance to a zero of $\det E(w)$ at a complex energy z_R such that $\mathrm{Re}\det E(w_R+i0)=0$, where $\mathrm{Re}z_r\simeq w_R$. Near w_R we may write $\mathrm{Re}\det E(w+i0)=c(w_R-w)$, $c=$constant, and

$$G_{ij}(w)=\frac{\mathfrak{R}_{ij}(w_R)}{c(w_R-w)+i\,\mathrm{Im}\det E(w_R+i0)}, \quad (3.13)$$

$$\mathrm{Im}G_{ij}(w)=\frac{\mathrm{Re}\mathfrak{R}_{ij}(w_R)}{c}\frac{\Gamma/2}{(w_R-w)^2+(\Gamma/2)^2}, \quad (3.14)$$

where $\Gamma/2=-\mathrm{Im}\det E(w_R+i0)/c$. With one minor exception, mentioned in the following section, the resonances of our theory are sufficiently narrow so that Eq. (3.14) is an acceptable approximation.

TABLE I. Positions and widths in units of the pion mass (139.6 MeV) as functions of the parameter x. Quantities in parentheses in the last row are the corresponding experimental numbers.

	$N^*_{3/2}$		Y^*_1		$\Xi^*_{1/2}$		Ω_0	
x	Position	Γ	Position	Γ	Position	Γ	Position	Γ
0.0	11.0	0.0	11.0	0.0	11.0	0.0	11.0	0.0
0.025	10.96	0.0	10.98	0.0	11.0	0.0	11.02	0.0
0.05	10.92	0.0	10.96	0.0	11.0	0.0	11.04	0.0
0.10	10.86	0.0	10.94	0.0	11.02	0.0	11.10	0.0
0.25	10.67	0.0	10.86	0.0	11.05	0.0	11.24	0.0
0.50	10.23	0.0	10.68	0.0	11.13	0.0	11.50	0.0
0.75	9.62	0.24	10.41	0.05	11.10	0.0	11.71	0.0
1.00	9.02	1.06	10.09	0.31	11.09	0.07	12.01	0.0
	(8.87)	(0.72)	(9.92)	(0.36)	(10.96)	(0.05)	(12.07 $\pm$0.09)	(0.0)

The Eq. (3.14) can also be used to define effective coupling constants of decuplet states to meson-baryon states. If one treats the resonant states as though they had infinitely narrow width, the contribution of a resonance to a dispersion integral can be evaluated by treating it as a pole at the mass of the resonance. By comparing the residue of this pole with the corresponding residue in the Born approximation of an appropriate Lagrangian, the conventional coupling constant is related to the resonance parameters.[18] We take the Lagrangian density

$$G_{B^*BP}\tfrac{1}{2}(\partial_\mu\bar{\psi}\phi-\bar{\psi}\partial_\mu\phi)\Psi^\mu+\text{H.c.} \tag{3.15}$$

where ψ, ϕ, and Ψ^μ correspond to baryon, meson, and decuplet fields, respectively. Isopin is suppressed. Ψ^μ is a Rarita-Schwinger field. We find for the coupling of a decuplet state B^* to pseudoscalar meson P and baryon B

$$\frac{G_{B^*BP}{}^2}{4\pi}=\frac{12w_R{}^2}{(w_R+M)^2-m^2}\frac{\mathrm{Re}\mathfrak{N}_{ii}}{c}\beta_i, \tag{3.16}$$

where $\mathrm{Re}\mathfrak{N}_{ii}$ is computed from the diagonal matrix element G_{ii} for $B+P\to B+P$ according to Eq. (3.14). β_i is the appropriate isotopic spin factor. From the explicit Lagrangian given by Martin and Wali,[19] one can find the ratios of the decuplet coupling constants in the limit of exact SU(3). The quantity of particular experimental interest, the Y_1^* branching ratio, is given by

$$\frac{Y_1^*\to\Sigma+\pi}{Y_1^*\to\Lambda+\pi}=\frac{2}{3}\frac{(\mathrm{Re}\mathfrak{N})_{\Sigma\pi}}{(\mathrm{Re}\mathfrak{N})_{\Lambda\pi}}\frac{(q_R)_{\Sigma\pi}{}^3}{(q_R)_{\Lambda\pi}{}^3}. \tag{3.17}$$

In the numerical evaluation of the theory we obtained precise values for the zeros w_R of $\mathrm{Re}\det E(w+i0)$, and then observed that nearly the same zeros could be obtained from the factored approximation (3.12). The lowest order corrections to the approximate zeros may be obtained as follows. Let w_A be an approximate zero; i.e., a zero of $E_{11}(w)$, where we have taken the index 1 to correspond to the 10 representation. Then

$$\det E=\begin{vmatrix}\beta(w_A-w) & \delta_{12} & \delta_{13}\cdots\delta_{1n}\\ \delta_{21} & \alpha_2 & \delta_{23}\cdots\delta_{2n}\\ \delta_{31} & \delta_{32} & \alpha_3\cdots\delta_{3n}\\ \vdots & \vdots & \vdots\cdots\vdots\\ \delta_{n1} & \delta_{n2} & \delta_{n3}\cdots\alpha_n\end{vmatrix}. \tag{3.18}$$

One finds that $|\delta/\alpha|<0.1$ over the energy range of interest. To lowest order in δ/α, the correction to the approximate zero w_A is

$$\Delta w_A=-\frac{1}{\beta}\left[\frac{\delta_{12}{}^2}{\alpha_2}+\frac{\delta_{13}{}^2}{\alpha_3}+\cdots+\frac{\delta_{1n}{}^2}{\alpha_n}\right]. \tag{3.19}$$

Another interesting way to analyze $\det E$ is by approximating the eigenvalues of E, since we know the eigenvalues in the case of pure symmetry. We solve the secular equation $\phi(\mu)=\det(E-\mu 1)=0$ by Newton's method. A first approximation is simply $\mu_i=E_{ii}=\alpha_i$, since (3.9) suggests that off-diagonal elements of E are

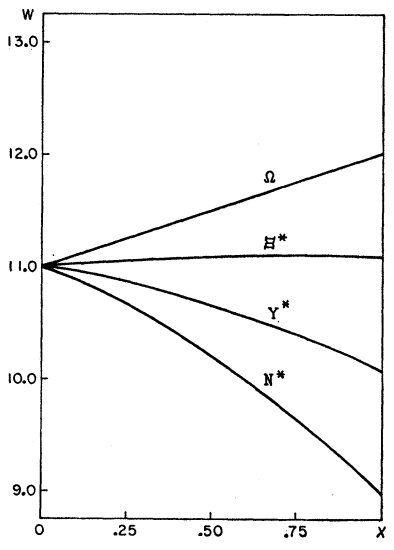

FIG. 2. The positions of the decuplet states plotted as a function of the parameter x.

[18] E. Abers and C. Zemach, Phys. Rev. **131**, 2305 (1963).
[19] A. W. Martin and K. C. Wali, Nuovo Cimento **31**, 1324 (1964).

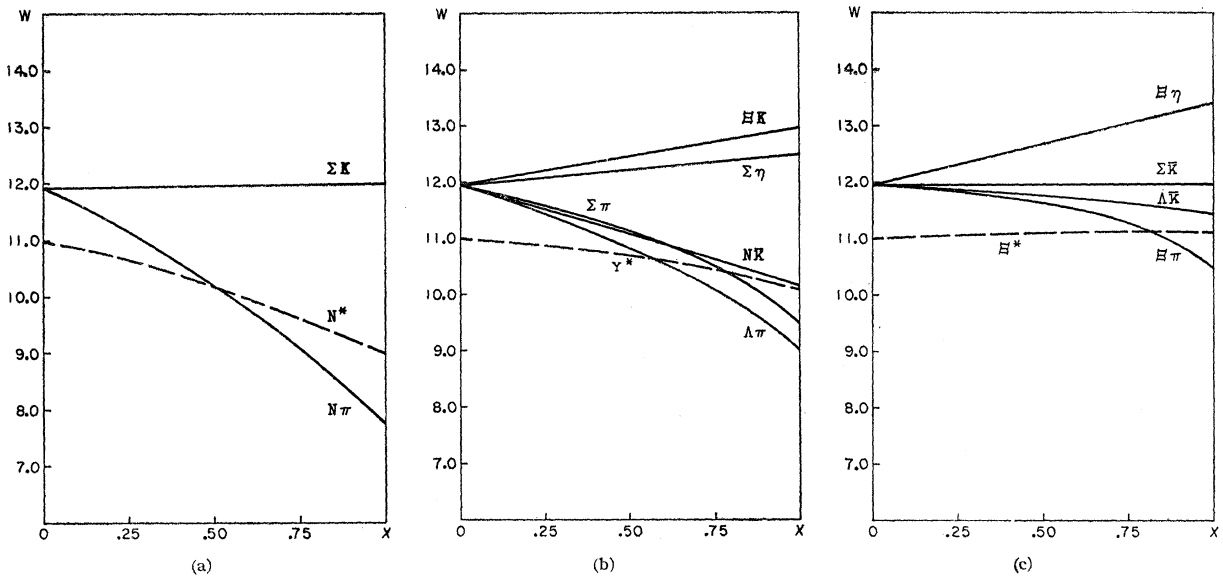

FIG. 3. (a)–(d). The positions of the poles corresponding to the decuplet states relative to the thresholds of their respective coupled channels plotted as a function of the parameter x.

not so very important. Expanding about α_i, we have

$$\phi(\mu)=\phi'(\alpha_i)\left(\mu-\alpha_i+\frac{\phi(\alpha_i)}{\phi'(\alpha_i)}+\cdots\right). \quad (3.20)$$

The first correction $-\phi/\phi'=-1/(\ln\phi)'$ may be calculated from the formula $\ln\det A=\mathrm{tr}\ln A$. Thus,

$$\mu_i=E_{ii}-\frac{1}{\mathrm{tr}(E_{ii}-E)^{-1}}+\cdots. \quad (3.21)$$

4. NUMERICAL RESULTS AND CONCLUSIONS

It was stated in the previous section that for fixed masses of the constituent particles the free parameters of our model are the $D-F$ mixing ratio determined by the parameter f, the subtraction point energy $\hat{w}$, and an over-all coupling constant $g^2/4\pi$. We choose the parameters so that the calculated decuplet states correspond closely to the observed ones when the constituent mesons and baryons have their observed masses. Taking account of the results of Ref. 6, we choose the parameter f to be 0.35; this ensures that the decuplet representation is the only one that is resonant in the low-energy region. Then with $\hat{w}=3m_\pi c^2$ and $g^2/4\pi=19$, the decuplet state energies agree fairly well with observation. We wish to emphasize that the approximately uniform level spacing (i.e., the validity of the Okubo formula) is substantially independent of the parameters, provided the resonances appear at all. The average value of the level spacings depends mostly on $\hat{w}$. This is only reasonable, since variations of $\hat{w}$ change the relative strengths of the different left-hand singularities, and hence the range of the attractive forces responsible for the resonance.

We characterize the symmetry violation by means of a parameter x, $0\leq x\leq 1$, introduced directly in the mass formula. For baryons,

$$M=M_0[1+xaY+xb(I(I+1)-Y^2/4)]. \quad (4.1)$$

When $x=1$, $M(I,Y)$ takes on the observed values; $x=0$ corresponds to exact symmetry. The constants a and b are known, and $M_0=M_\Lambda$. For mesons one has a similar formula for masses squared.

$$m^2=m_0^2[1+xa'Y+xb'(I(I+1)-Y^2/4)], \quad (4.2)$$

where $m_0^2=m_\eta^2$.

Table I gives the calculated resonance or bound-state positions and widths and the corresponding experimental values. It also gives the positions and widths as functions of x. In this table and in the following energies are given in units of $m_\pi c^2$ (139.6 MeV). The positions

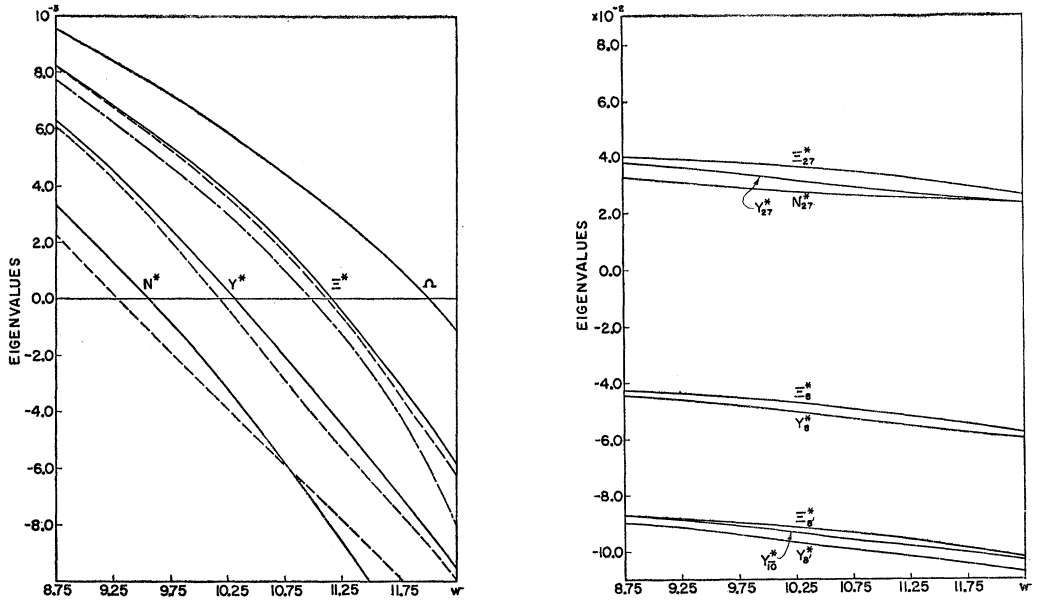

FIG. 4. (a) The eigenvalues corresponding to the 10-fold representation plotted as a function of the energy w. The particle labels used on these curves are merely to indicate the quantum numbers of the coupled channels in which they appear. The dashed curves represent the eigenvalues evaluated including only the perturbations of the diagonal elements [Eq. (3.12)]. The solid curves represent the same eigenvalues evaluated by using the approximation given by Eq. (3.21). The long dash-short dash curve represents the limit of these curves in the unperturbed situation. (b) The "nonresonant" eigenvalues corresponding to the indicated representations plotted as a function of the energy w.

are plotted as functions of x in Fig. 2, which shows that the Okubo equal spacing rule is satisfied to reasonable accuracy. The spacings become more nearly equal as x is decreased. The calculated widths agree well enough with experiment, except in the case of $N_{3/2}$*. The $N_{3/2}$* width being too large seems to be typical of theories based on single baryon exchange.

For the branching ratio $R=(Y_1^* \to \Sigma+\pi)/(Y_1^* \to \Lambda+\pi)$ we calculated 0.10 from formula (3.17). This figure is to be compared to $R=0.20$, which is obtained from (3.17) if the factor $(\mathrm{Re}\mathfrak{N})_{\Sigma\pi}/(\mathrm{Re}\mathfrak{N})_{\Lambda\pi}$ is set equal to one.[20] The departure of this factor from one represents effects of symmetry breaking beyond those involved in q^3 phase-space factors. These effects were ignored in earlier estimates of the branching ratio.[21]

Figures 3(a) through 3(d) show the courses of the levels as compared to the courses of the thresholds. The energies plotted are the values of w_R for which $\mathrm{Re}\,\det E(w_R+i0)=0$. The motion of a resonance in crossing a threshold is perfectly smooth and presents no problem of the type discussed by Oakes and Yang.[9]

A word about the definition of resonance position is in order. Instead of our definition one could take $\det \mathrm{Re}E(w_R+i0)=0$, as suggested by Dalitz.[22] The position of the peak of the scattering cross section might be taken as a third definition. In the present calculation the three energies differ negligibly for Y_1* and $\Xi_{1/2}$*, and all lie within an interval of 15 MeV in the case of $N_{3/2}$* at $x=1$. For $N_{3/2}$* the difference between the zero of $\mathrm{Re}\,\det E$ and the peak of the cross section means a slight inaccuracy in Eq. (3.14).

The eigenvalues μ_i of the matrix E were computed in the approximation (3.21), over a range of energies.[23] Their real parts are shown in Figs. 4(a) and 4(b), for $x=1$. The diagonal elements $\mathrm{Re}E_{ii}$, which form the zeroth order approximations to the $\mathrm{Re}\mu^i$, are also plotted. As was mentioned in the preceeding section, E factorizes in the limit of exact symmetry. Each factor corresponds to an irreducible representation of SU(3). The quantities $\mathrm{Re}\mu_i$ are proportional to the cotangents of the eigen phase shifts, with or without symmetry breaking. Our choice of the $D-F$ mixing parameter is such that in the pure symmetry case only the phase corresponding to the 10 representation passes through

[20] These two values for R were both calculated at $w=10.085$, the energy of Y_1* in our theory. Better agreement with the experimental indications (Ref. 3) that $R<0.05$ would be obtained if the parameters of the theory were altered to put Y_1* at exactly its observed position $w=9.92$. This is because $(q^3)_{\Sigma\pi}/(q^3)_{\Lambda\pi}$ increases rapidly with energy. If we calculate this momentum ratio at $w=9.92$, but keep the same value for the slowly varying factor $(\mathrm{Re}\mathfrak{N})_{\Sigma\pi}/(\mathrm{Re}\mathfrak{N})_{\Lambda\pi}$ that it had at $w=10.085$, we obtain $R=0.07$.

[21] S. L. Glashow and J. J. Sakurai, Nuovo Cimento **25**, 337 (1962).

[22] R. H. Dalitz, Rev. Mod. Phys. **33**, 471 (1961).

[23] The approximation (3.21) is not extremely accurate, as can be seen from the poor values for the resonance positions obtained from the approximate eigenvalues. We nevertheless believe that the accuracy is sufficient for our purposes, since $\det E$ agrees well with $\Pi_{i=1}{}^n \mu_i$, except very near the resonances where both quantities are small.

TABLE II. $|U^\dagger GU|^2$ at resonance positions. The normalization is such that $|(U^\dagger GU)_{10,10}|^2=1$.

$N_{3/2}$*

	10	27
10	1	3.8×10^{-2}
27		4.4×10^{-3}

Y_1*

	8	8′	10	$\overline{10}$	27
8	2.8×10^{-4}	7.6×10^{-9}	1.2×10^{-4}	5.1×10^{-8}	1.2×10^{-6}
8′		7.5×10^{-5}	6.9×10^{-5}	2.6×10^{-8}	1.7×10^{-6}
10			1	3.8×10^{-5}	1.7×10^{-2}
$\overline{10}$				8.0×10^{-5}	5.0×10^{-8}
27					6.7×10^{-4}

$\Xi_{1/2}$*

	8	8′	10	27
8	1.0×10^{-5}	2.8×10^{-10}	1.8×10^{-5}	6.5×10^{-8}
8′		3.0×10^{-6}	6.2×10^{-5}	3.7×10^{-7}
10			1	5.2×10^{-3}
27				4.8×10^{-5}

$\pi/2$. From Fig. 4 it is clear that this feature persists when the mass differences are introduced. The 10 eigenvalues split apart, as expected, giving the level spacings. The other eigenvalues exhibit smaller splittings and remain large throughout the energy range considered. Therefore, we are justified in associating the resonant states with the 10-dimensional representation, even when when the symmetry is broken. From Fig. 4(a) and Table I it is seen that the zeros of the appropriate diagonal elements $\mathrm{Re}E_{ii}$ agree roughly with the actual level positions. This fact was already indicated in Eq. (3.12). However, it is interesting to note Eq. (3.19), which shows that this agreement will be less if the nonvanishing diagonal elements of E are reduced in magnitude.

In the face of substantial symmetry breaking the meaning of group invariance arguments is not well defined. Perturbations may affect different types of observables in different degrees. Besides finding the perturbations of eigen phase shifts, we have considered some other ways of judging the degree of symmetry violation. The various ways are closely related, but they serve to point up different aspects of the situation.

In Table II we list the squared absolute values of the transition amplitudes in the unitary spin representation; i.e., $|(U^\dagger GU)_{\alpha\beta}|^2$ for $x=1$. As expected, the nonresonant diagonal elements are small. The off-diagonal elements (which are zero in the case of exact symmetry) are of the same order as the nonresonant diagonal terms. The 10–27 transition is by far the largest of the off-diagonal processes, which suggests that the main symmetry breaking effects could be attributed to 10–27 mixing.

To determine the mixtures of various representations in the resonant states, we diagonalize the imaginary part of the matrix of residues of G at the resonance pole. Actually, we diagonalize the matrix $\mathrm{Re}\mathfrak{N}(w_R+i0)$ defined in Eq. (3.13); for narrow resonance width, this is essentially the same as the imaginary part of the residue matrix. The diagonalization is a trivial operation, since $\mathrm{Re}\mathfrak{N}$ is practically degenerate: $\mathrm{Re}\mathfrak{N}_{ij}\simeq v_i v_j$. This fact, which is familiar from the theory of nuclear reactions, may be proved very simply by means of the ND^{-1} representation. We have $\mathfrak{N}=G\det E$, so $\det\mathfrak{N}=(\det E)^n\det G$ if there are n channels. But $\det G=\det(N\Lambda^{-1}/\det E$, so $\det\mathfrak{N}$ has a zero of order $n-1$, where $\det E$ vanishes. Thus, $\mathfrak{N}$ has rank 1 at the pole, and consequently every 2×2 subdeterminant of $\mathfrak{N}$ vanishes. By considering 2×2 subdeterminants of the type

$$\begin{vmatrix}\mathfrak{N}_{ii} & \mathfrak{N}_{ij}\\ \mathfrak{N}_{ji} & \mathfrak{N}_{jj}\end{vmatrix}=0,$$

we find that $\mathfrak{N}_{ij}=v_i v_j$, because of the symmetry $\mathfrak{N}_{ij}=\mathfrak{N}_{ji}$. If w_P is the pole position, and w_R is the corresponding point on the real axis where $\mathrm{Re}\det E(w_R+i0)=0$, we have $\mathfrak{N}(w_P)\simeq\mathfrak{N}(w_R+i0)$. Numerical evaluation of $\mathfrak{N}(w_R+i0)$ shows that $\mathrm{Im}\mathfrak{N}(w_R+i0)\ll\mathrm{Re}\mathfrak{N}(w_R+i0)$. This latter circumstance is essentially the statement that the imaginary parts of the integrals occurring in E are much less than the corresponding real parts. Thus, $\mathrm{Re}\mathfrak{N}_{ij}(w_R+i0)\simeq\mathfrak{N}_{ij}(w_P)=v_i v_j$, and $v_i\simeq v_i^*$. The factorization of $\mathrm{Re}\mathfrak{N}_{ij}$ holds numerically to excellent accuracy. The eigenvector of $\mathrm{Re}\mathfrak{N}$ corresponding to the one nonzero eigenvalue is $\mathbf{v}=[v_i]$. Since $\mathfrak{N}$ was defined as a matrix in the particle representation, the v_i are the "probability amplitudes" for finding various particle states in the resonant state. Of course, since certain channels are closed, v_i^2 does not have direct observational significance. It merely represents the closest mathematical analog to a probability for decay into particle channel i. We state the results in Table III for $x=1$. The channels with thresholds lying close to the resonance energy are generally enhanced with respect to exact SU(3) predictions, while the channels with distant thresholds are depleted. The $\Sigma\pi$ channel does not follow this rule.

Alternatively, we may write $(U^\dagger\,\mathrm{Re}\mathfrak{N}U)_{ij}\simeq u_i u_j$, where the components of $\mathbf{u}=[u_i]$ are the probability amplitudes for finding group representation states in the resonant state. We express the resonant state $|\psi\rangle$

TABLE III. "Probabilities" for broken and unbroken symmetry.

	"Probabilities" v_i^2	v_i^2 by exact SU(3)
$T=\frac{3}{2}, Y=1$		
$N\pi$	68.20%	50%
ΣK	31.80	50
$T=1, Y=0$		
$\Lambda\pi$	31.84	25
$\Sigma\pi$	15.97	16.67
$N\bar{K}$	21.82	16.67
$\Sigma\eta$	18.00	25
ΞK	12.37	16.67
$T=\frac{1}{2}, Y=-1$		
$\Xi\pi$	26.19	25
$\Lambda\bar{K}$	30.33	25
$\Sigma\bar{K}$	22.84	25
$\Xi\eta$	20.64	25

TABLE IV. Ratios of the coupling constants as a function of the parameter x.

$g^2_{B^*BP}$ / $g^2_{N^*N\pi}$	x 0.0	0.025	0.05	0.1	0.25	0.5	0.75	1
$N^*N\pi$	6.0	6.0	6.0	6.0	6.0	6.0	6.0	6.0
$N^*\Sigma K$	6.0	5.87	5.75	5.50	4.80	3.76	2.90	2.34
$Y^*\Lambda\pi$	3.0	3.02	2.95	2.90	2.88	3.10	2.35	1.82
$Y^*\Sigma\pi$	1.0	0.992	0.962	0.933	0.871	0.857	0.601	0.431
$Y^*N\bar{K}$	1.0	1.01	0.988	0.981	0.993	1.12	0.905	0.750
$Y^*\Sigma\eta$	3.0	2.97	2.86	2.72	2.47	2.28	1.48	1.01
$Y^*\Xi K$	1.0	0.988	0.950	0.906	0.813	0.738	0.467	0.310
$\Xi^*\Xi\pi$	1.0	0.980	0.957	0.941	0.877	0.880	0.633	0.403
$\Xi^*\Lambda\bar{K}$	3.0	2.95	2.91	2.92	2.85	3.06	2.41	1.68
$\Xi^*\Sigma\bar{K}$	1.0	0.979	0.953	0.934	0.862	0.854	0.613	0.399
$\Xi^*\Xi\eta$	3.0	2.90	2.83	2.76	2.49	2.34	1.63	0.987
$\Omega\Xi\bar{K}$	6.0	5.91	5.66	5.52	5.16	5.25	3.79	2.42

as a normalized linear combination of the group states.

$$T=\tfrac{3}{2},\ Y=1$$
$$|\psi\rangle=0.98|10\rangle+0.18|27\rangle,$$
$$T=1,\ Y=0$$
$$|\psi\rangle=0.99|10\rangle+0.13|27\rangle+0.008|8'\rangle+0.003|\bar{10}\rangle+0.0007|8\rangle,$$
$$T=\tfrac{1}{2},\ Y=-1$$
$$|\Psi\rangle=0.997|10\rangle+0.07|27\rangle+0.007|8'\rangle+0.001|8\rangle. \quad (4.3)$$

It is important to remember that in these formulas the states on the right represent linear combinations [with coefficients given by exact SU(3) symmetry] of definite particle states with physical masses. As was already apparent in Table II, the principal contamination of the 10 representation comes from the 27. However, the mixing is small enough so that there is no doubt about associating the resonance primarily with the 10 representation. Tarjanne and Cutkosky[7] obtained much larger mixing in a calculation which is difficult to compare with ours. Note that we have diagonalized the residue of $G_{ij}=T_{ij}/q_iq_j$. Had we not factored out q_iq_j, the symmetry might have been less apparent. In any case, our model certainly proves the existence of a set of left singularities which imply both the observed decuplet mass differences and relatively small mixing, provided the mixing is measured in the way specified. In judging the degree of mixing, it is appropriate to consider directly the coefficients of Eq. (4.3), rather than their squares. For example, in the case $T=\frac{3}{2}$, $Y=1$, a comparison of $(0.98)^2$ with $(0.18)^2$ might suggest that the amount of $|27\rangle$ is negligible. However, from $|10\rangle=2^{-1/2}(|\pi N\rangle-|K\Sigma\rangle)$ and $|27\rangle=2^{-1/2}(|\pi N\rangle+|K\Sigma\rangle)$ it follows that $(v_{\pi N}/v_{K\Sigma})^2=[(0.98+0.18)/(0.98-0.18)]^2=2.1$. This ratio, which is unity in the case of no 10–27 mixing, is involved in $g^2_{N^*N\pi}/g^2_{N^*\Sigma K}$.

Finally, we discuss the coupling constants defined by Eq. (3.16). Although the properties of these constants are roughly similar to those of the v_i^2, the two sets of constants are related by factors in which appreciable effects of symmetry breakdown are manifest. For each x we compute $g^2_{B^*BP}$ in units such that $g^2_{N^*N\pi}=6.0$. The results are shown in Table IV. For large values of x the ratios deviate considerably from the values given by exact symmetry. The deviations do not agree with the sum rules of Dullemond *et al.*[8] and Sudarshan,[8] even at the smaller x values.

ACKNOWLEDGMENTS

We wish to acknowledge the generous and expert help of Mary Wrenn, who advised us in programming the IBM-7090 computer at the IIT Research Institute.

We should also like to thank Professor E. C. G. Sudarshan for helpful discussions of the coupling constant sum rules.

APPENDIX: QUANTITATIVE STUDY OF POLES IN A TWO-CHANNEL EXAMPLE

In order to make perfectly explicit the observations of Sec. 2, we calculate the positions of poles on all sheets in a simple, two-channel problem. We wish to illustrate the phenomenon of a resonance crossing a threshold other than the lowest threshold of the problem. The $\pi N-K\Sigma$ problem of the last section is not suitable for this purpose, since the $N_{3/2}$* crosses only the lower threshold. The latter crossing occurs merely by the pole on the $(-+)$ sheet passing through the threshold. To obtain a case in which a resonance crosses the upper threshold, we modify the $\pi N-K\Sigma$ problem by reducing the coupling constant so that $N_{3/2}$* moves up to an energy just below the $K\Sigma$ threshold. Then, as the symmetry-breaking parameter x is reduced, the resonance moves upward through the $K\Sigma$ threshold.

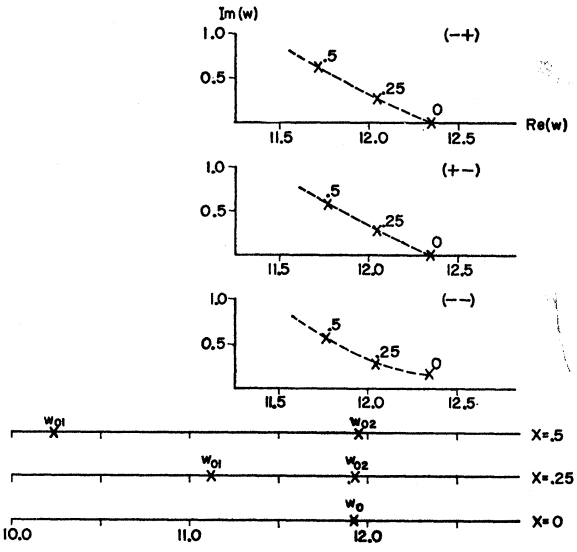

FIG. 5. The positions of the poles on the unphysical Riemann sheets for $0\leq x\leq 0.5$. The corresponding values for the channel thresholds are shown at the bottom.

We take only the values $x=0.5$, 0.25, and 0; for larger x the resonance width becomes ridiculously large. With $g^2/4\pi=12.8$ and $x=0.5$, we have $w_{01}=10.23$, $w_{02}=11.95$, and $w_R=11.72$, in units of the pion mass. As x goes to zero, the thresholds coalesce at $w_0=12.35$.

The trajectories of the poles on the three unphysical sheets are plotted in Fig. 5. The positions of the thresholds for each x are shown (on the same energy scale) below the graphs. As was expected, for each x there is a pair of complex conjugate poles on each of the sheets; the graphs show just the member of each pair that lies in the upper half-plane. For $x=0.5$, the poles have nearly identical positions on the various sheets, and the resonance peak is due to the poles on sheet $(-+)$. For $x=0.25$, the poles again have similar positions on all three sheets, but the resonance has crossed the threshold. The peak is now mainly associated with the poles on sheet $(--)$. In the degenerate limit $x=0$ the "original" resonance poles of $(-+)$ have moved onto the real axis of $(-+)$. Since $(-+)$ is now completely inaccessible from the physical sheet $(++)$, this pole has no physical effect whatever. The same may be said of the poles on $(+-)$, which have also moved onto the real axis. The poles on $(--)$ end up at $w=12.35\pm0.16i$, and therefore represent a resonance with half-width $\Gamma/2=0.16$.

The pole positions as shown in Fig. 5 were calculated in the usual approximation that takes advantage of the fact that the poles are all close to the real axis. If $E^{(\alpha)}$ is the E matrix on sheet (α), then near a zero w_R of $\mathrm{Re}\,\det E^{(\alpha)}$ we have

$$\det E^{(\alpha)}(w\pm i0)=c(w_R-w)\pm i\,\mathrm{Im}\,\det E^{(\alpha)}(w_R+i0)$$

and the poles on sheet α are at

$$w\approx w_R\pm i(1/c)\,\mathrm{Im}\,\det E^{(\alpha)}(w_R+i0).$$

We list the formulas for $\det E^{(\alpha)}(w\pm i0)$ for w on and just below the right-hand physical cut. $\mathcal{E}$ stands for $\mathrm{Re}\,\det E(w+i0)$, and $\lambda^{-1}=\frac{1}{2}(\lambda_1^{-1}+\lambda_2^{-1})$, where the λ_i are the eigenvalues of N_0 as defined in Eq. (3.5). The integrals I_i are defined by

$$I_i(w)=-\frac{w-\hat{w}}{\pi}\int_P\frac{\rho_i(w')h(w')dw'}{(w'-\hat{w})(w'-w)},$$

and the other notations are as in Sec. 3.

Sheet $(-+)$

$w<w_{01}$: $\mathcal{E}+2|q_1|^3h(I_2+\lambda^{-1})$

$w_{01}<w<w_{02}$: $\mathcal{E}\pm iq_1^3h(I_2+\lambda^{-1})$

$w>w_{02}$: $\mathcal{E}+(q_1q_2)^3h^2$
$\pm ih[q_1^3(I_2+\lambda^{-1})-q_2^3(I_1+\lambda^{-1})]$;

Sheet $(+-)$

$w<w_{01}$: $\mathcal{E}+2|q_2|^3h(I_1+\lambda^{-1})$

$w_{01}<w<w_{02}$: $\mathcal{E}+|q_2|^3h(I_1+I_2+2\lambda^{-1})$
$\mp iq_1^3h(2|q_2|^3h+I_2+\lambda^{-1})$

$w>w_{02}$: $\mathcal{E}+(q_1q_2)^3h^2$
$\mp ih[q_1^3(I_2+\lambda^{-1})-q_2^3(I_1+\lambda^{-1})]$;

Sheet $(--)$

$w<w_{01}$: $\mathcal{E}+4|q_1q_2|^3h^2$
$+2h[|q_1|^3(I_1+\lambda^{-1})+|q_2|^3(I_2+\lambda^{-1})]$

$w_{01}<w<w_{02}$: $\mathcal{E}+|q_2|^3h(I_1+I_2+2\lambda^{-1})$
$\pm iq_1^3h(2|q_2|^3h+I_2+\lambda^{-1})$

$w>w_{02}$: $\mathcal{E}-(q_1q_2)^3h^2$
$\pm ih[q_1^3(I_2+\lambda^{-1})+q_2^3(I_1+\lambda^{-1})]$.

From these formulas one can check that the sheets are connected as shown in Fig. 1; e.g., $\det E^{(-+)}(w\pm i0)=\det E^{(+-)}(w\mp i0)$ for $w>w_{02}$, so $(-+)$ and $(+-)$ are connected along the real axis above the second threshold.